

Supersaturation Controlled Wet Synthesis of Nanohydroxyapatite for Biological Applications

GS Dhananjaya#, TGD Madusanka and SU Adikary

Department of Material Science and Engineering, University of Moratuwa, Sri Lanka

#eng.gs.dhana@gmail.com

Abstract— In this study, the effect of supersaturation for wet chemical synthesis of Nano-hydroxyapatite HA $[\text{Ca}_{10}(\text{PO}_4)_6(\text{OH})_2]$ was investigated. The nano-hydroxyapatite powder was synthesized using $\text{Ca}(\text{OH})_2$ and H_3PO_4 as precursors at five different supersaturations while the temperature for the whole study remained at 30°C . The supersaturation for hydroxyapatite was caused by changing the concentration of precursors maintaining the constrained molar ratio near 1.67 between Calcium and Phosphorus Ca/P. The H_3PO_4 was added to the $\text{Ca}(\text{OH})_2$ suspension at a constant acid addition rate of 4ml/min using a burette under vigorous stirring having maintained the final pH at 10. During the synthesis, the variation of pH of the mixed precursor suspension was measured and analysed. After 48 h aging, the precipitate was separated by centrifuging at room temperature. Then the resulting wet powder samples were dried and characterized. The particle size distribution was obtained by Laser Particle Size Analyzer and Fourier Transform Infrared (FTIR) spectroscopy investigated the bonding structure of pure hydroxyapatite. In addition to that, morphological and chemical analysis was done by Scanning Electron Microscopy (SEM). As a measurement, the time taken by the final precursor mixture to start reducing pH value increased with the supersaturation decreasing. It was clearly observed that the particle size and the standard deviation of the distribution or a broader distribution had increased with decreasing supersaturation. Finally, this model could be used to predict the particle size distribution of hydroxyapatite resulting from a wet chemical routine with the supersaturation which depends basically upon precursor concentrations.

Keywords: *nano-hydroxyapatite, wet chemical precipitation, supersaturation, particle size distribution*

I. INTRODUCTION

Recently, different phosphates of calcium are the materials being used for a variety of medical applications like controlled drug formulation and delivery, tissue engineering, and implants in dentistry as mentioned by Uskoković and Wu (2016). Apart from the medical applications, hydroxyapatite is used in fuel cells (Gross, Berndt, et al. 1998) and column chromatography as packing material (Morales, Burgues, et al. 2001) Among calcium phosphates, Naruporn M (2008) expressed the views on hydroxyapatite as a bioactive and biocompatible ceramic which has a similar mineral structure and composition to the naturally occurring hard tissue in bone and teeth of humans. Materials having higher crystallinity and chemical stability like hydroxyapatite are good candidates to be a productive biomaterial. With respect to mechanical properties, hydroxyapatite (HA) has poor hardness, low tensile strength, low compressive strength which makes it suitable for applications that require little or no-load bearing functionality as described by Liu and Troczynski (2001). Naruporn M (2008) reviews that there is a broader diversity of preparation methods of hydroxyapatite like solid state synthesis, hydrothermal methods, sol-gel methods, electro crystallization, sonochemical synthesis, spray pyrolysis and wet chemical precipitation. Although there are so many techniques to synthesis hydroxyapatite, *Guzm'an V' azquez, et al* (2005) emphasized that the wet chemical precipitation method is the most predominant one in terms of the ease of experimental procedure, lower synthesis temperature, yield, and cost of required equipment.

However, the diversified application of hydroxyapatite needs to be tailored based on the application. Basically, different researchers all over the world have altered and customized its properties such as stoichiometry, size and distribution, tensile properties, morphology, sinterability and solubility. As Sudip and Apurba (2016) states, the property customization can be done by varying the synthesis methodology along with controlling parameters such as pH, precursors and their concentrations, temperatures, etc. Based on the parameters above mentioned, some

mathematical and kinetic models have been established depending upon kinetics (Thanh, Maclean, et al. 2014). As they derived analytically based on the classical nucleation theory, the nucleation rate is basically a function of temperature and supersaturation.

For spherically nucleating particles, the homogeneous nucleation rate is given by,

$$\frac{dN}{dt} = A \exp\left(-\frac{16\pi v^2 \gamma^3}{3(k_B T)^3 (\ln(S))^2}\right) \dots\dots (1)$$

where, the nucleation rate, dN/dt is dependent upon pre-exponential factor A , molar volume v , interfacial energy between the growing phase and solution γ , Boltzman's Constant k_B , absolute temperature T , and Supersaturation S .

Supersaturation gives an indication about how many times the ionic activity product is greater than the activity product in its saturation.

$$S = Q/K_{sp} \dots\dots (2)$$

where, Q is the ionic activity product of precursor ions in the solution for the given stoichiometry (Dragan, Vuk et al. 2010)

The Q was calculated by considering ionic activities of Ca^{2+} , PO_4^{3-} and OH^- in the solution as given in EQ03

$$Q = [a_{Ca^{2+}}]^5 [a_{PO_4^{3-}}]^3 [a_{OH^-}] \dots\dots (3)$$

In medical implantations and orthopedic and orthodontic application in tissue engineering like scaffolds, the medical grade hydroxyapatite must be osteoconductive, which means it must be compatible with hard tissue in the body for the continuum (Ferraz, Monteiro, et al. 2004). For the osteoconductivity, two major important factors are particle size and purity of the hydroxyapatite synthesized. Nano size and wet chemical precipitation is thereby preferred for biological grade hydroxyapatite. Therefore, in this research work, the wet chemical process was chosen for the synthesise of hydroxyapatite particles additionally because it offers a molecular level of mixing to improve the chemical homogeneity of the product which affects the uniformity of nucleation. Basically, this study focused on the particle size and its distribution depending upon the supersaturation which was calculated based on concepts from analytical chemistry. Although there are so many studies in the literature to have a nano-size particle distribution from different synthesis methods, the particle size tailored to the synthesis variable parameters has not been well established. Hence, the main objective of this work was to tailor

the particle size to precursor concentration based-parameter, supersaturation, leaving the working temperature, Ca/P molar ratio and acid addition rate constant.

II. METHODOLOGY

A. Chemicals and reagents

Analytical grade Calcium hydroxide [$Ca(OH)_2$, 98%] was procured from VWR, orthophosphoric acid [Assay (H_3PO_4), min 88%], ammonium hydroxide [NH_4OH , 28%], Ethanol [C_2H_5OH] were procured from MERCK Specialties Private Limited. During the synthesis, deionized water (DI) was used as the solvent.

B. Experimental procedure

As the Table 1 shows, five samples of from different precursor concentration (in $mol\,dm^{-3}$) were prepared.

Table 1. Precursors' concentration for five Samples.

Sample \ Reagent	1	2	3	4	5
$Ca(OH)_2$	0.1670	0.3400	0.6300	0.8400	1.0400
H_3PO_4	0.1000	0.2000	0.3710	0.4940	0.6000
Ca/P	1.67	1.7	1.70	1.70	1.73

First 250 ml suspension of $Ca(OH)_2$ was magnetically stirred for 1 h in a beaker. Then 250 ml of H_3PO_4 was poured in a burette and added dropwise to calcium hydroxide suspension with a flowrate of 4 ml/min under continuous mechanical agitation. After the completion of acid addition, the reactant mixture was subjected to ultrasonic stirring for 30 mins. Then, quick and dropwise addition of ammonia hydroxide was made to raise the reactant mixture pH to 10 under magnetic stirring. After setting the final pH to 10, pH was noted for every 30 second interval under mechanical agitation. After a time-independent and constant pH suspension was observed, mechanical agitation was stopped, and the sample was placed in 48 h aging. Then the water layer above the deposition was removed and the sample was centrifuged at 5000 rpm for 6 mins at 30 °C with DI water. Finally, the precipitation in centrifuging

tubes was carefully separated to a petri dish. One specimen of this wet precipitate was analyzed with laser particle analyzer (HMK-CD2, 0.02 - 2000 μm). This wet sample of synthesis was placed in the oven at 60 $^{\circ}\text{C}$ for 2 $\frac{1}{2}$ hr. Then, the resulting powder was diluted in ethanol and sonicated in order to prepare a drop cast for the SEM analysis. The molecular bond structure or the functional groups present in the hydroxyapatite powder was determined by Fourier transform infrared spectroscopy (Bruker Alpha-T) in the scanning range of 4000 - 400 cm^{-1} using a cold pressed pellet of KBr containing 1% hydroxyapatite.

III. RESULTS AND DISCUSSION

The supersaturations (S) for five samples were calculated and the values of $\ln(S)$ are graphically shown by the Figure 1.

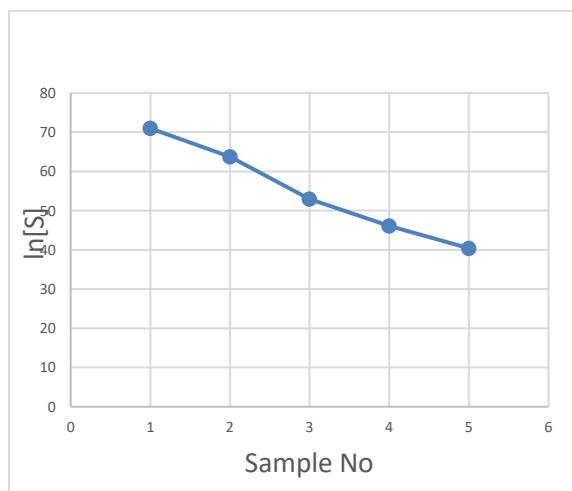
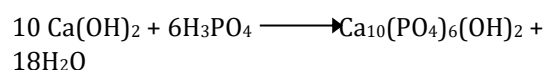


Figure 4. Calculated supersaturations for five Samples.

One may be surprised because in this study the highest supersaturations have been recorded by the sample with lowest precursor concentrations. In conventional calculations, the ionic interactions in highly charged suspensions are not considered. But in this study, all the analytical calculations were based on the electrostatic interactions that occur in solutions between the various charged ionic species. With high precursor concentrations, the electrostatic interactions are at maximum and it will reduce the totally decomposed ionic concentrations like PO_4^{3-} . Therefore, for the supersaturation calculations ionic strengths have been considered with Debye-Huckel equation for aqueous solutions. Accordingly, the highest ionic strength has shown by sample 05. Hence highest activity coefficients have shown in sample 01 giving rise to supersaturation.

With the dropwise acid addition to the calcium hydroxide suspension, the final pH of the mixture came near 6. Figure 2 shows the pH variation for the first synthesis after the pH adjustments of the final mixture to 10. It shows after 300 seconds, the first sample started to drop pH. According to the kinetic theory in classical nucleation, that rest time of the reaction is called the induction time (τ) and during that period nucleation takes place within the suspension. The chemical reaction taking place during the HA formation can be suggested as follows.



The formation of hydroxyapatite particles from the supersaturated solution consumes OH^- ions reducing the pH in the suspension.

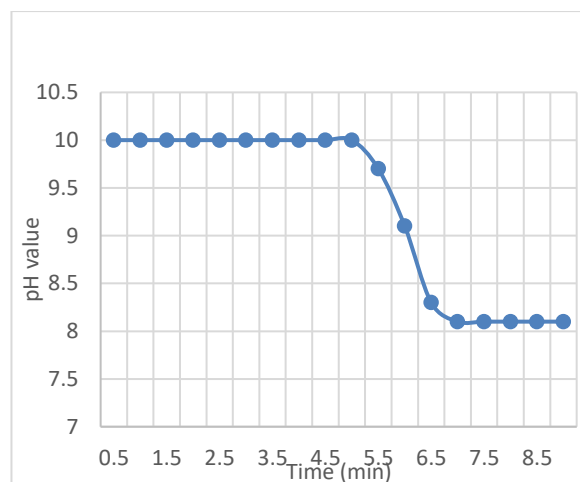


Figure 2. pH Variation with the reaction time of first Sample

As Figure 3 illustrates, the induction time has increased with reducing supersaturation. The least induction time was reported for the highest supersaturated solution 01. Dragan and Vuk et al (2010) modeled the nucleation rate in terms of induction time. As they suggested the induction time is a measure of nucleation rate which cannot be directly measured. It is obvious that with increased nucleation rates, the particle size will decrease which ultimately means that the lower induction time results in reduced particle sizes. This phenomenon will support the formation of reduced particle size with higher supersaturation.

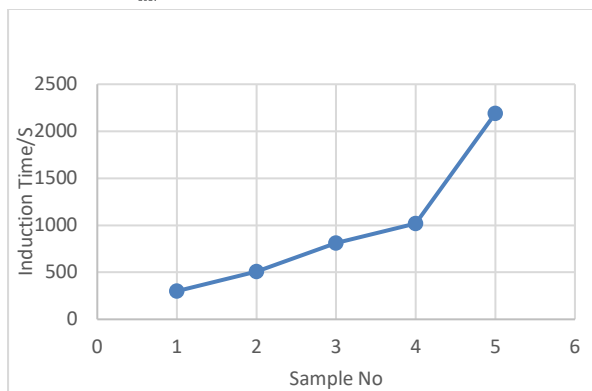


Figure 3. Variations of induction time for five samples

FTIR absorption spectrum of hydroxyapatite is shown in the Figure 4. As Sahebali Manafi and Seyyed (2008) concluded, the narrow bands located at around 472, 575, 963 cm^{-1} are attributed to the characteristic bands of PO_4^{3-} . The absorption band appeared at 472 cm^{-1} represents the ν_2 bending vibration. The narrow band near at 963 cm^{-1} corresponds to ν_1 vibration of PO_4^{3-} ions in hydroxyapatite. The absorption bands appeared at 575 cm^{-1} and 601 cm^{-1} can be attributed to the ν_4 fundamental bending mode of phosphate ions. The range of band appeared in between 1089-1036 cm^{-1} are dealt with ν_3 vibrations of phosphates. The band revealed around 1459 cm^{-1} is evident for the presence of a little amount of CO_3^{2-} in the sample as Tampieri and celotti (1997) showed. The IR absorption bands appeared around 3573 cm^{-1} and 632 cm^{-1} are stretching and vibration modes of OH- ions respectively present in the hydroxyapatite.

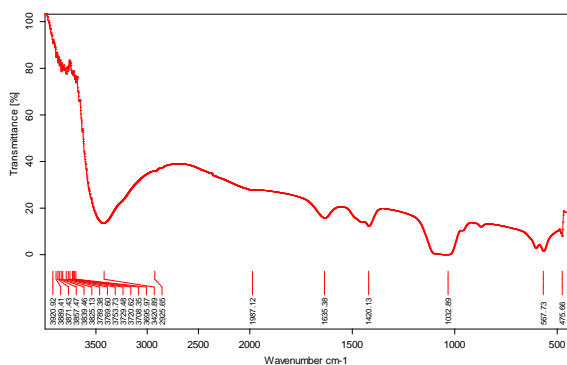
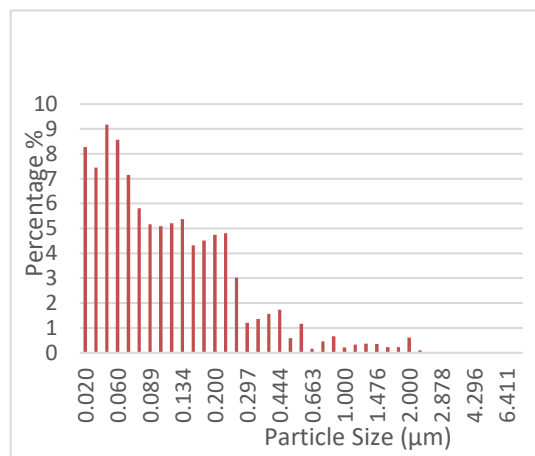


Figure 4. FTIR spectrum pattern of Synthesized first sample

Laser particle analyser recorded the particles beyond 20nm. This technique was selected because it gives the real particle size containing very small number of crystallites while powder x ray diffraction gives the crystallite size. The Figure 5-9 demonstrate the particle size distribution curves

obtained from the laser particle analyser. The mean and the stand deviation of each distribution are tabulated in Table 2. This experimental work basically focused on the nucleation rate which is inversely proportional to the induction time. But in the pH dropping period, the nucleated particles are growing up to the solubility limit of the hydroxyapatite. As the pK_{sp} value which is 117.3 at 37°C for HA suggests the growing of particles will predominantly occurs because the experiment deals with higher supersaturations. Therefore, the mode can be given as a good parameter to interpretate the particle size distributions obtained. Therefore, the lowest modal particle size was obtained for the first sample with highest supersaturation. This decrease in size with increasing supersaturation can collaboratively be explained by the above-mentioned nucleation theory. When the supersaturation is very high, the nucleation is promoted with higher nucleation densities leading to smaller particles and shorter induction time as the shortest induction time for the first sample. It can be considered as an experimental validation for the theoretical concepts generated. The distribution for the first sample is cut off from the left-hand side because it has the limitation of cut off size as 20 nm only. But the Gaussian curve is also established there. The Gaussian fitting is applicable for all distributions. The standard deviation has increased with sample number resulting in a broader distribution. This can be caused by the higher concentrations of precursors with loosing supersaturations after rapid nucleation. In broader distributions, particles



have grown to greater extent.

Figure 5. Laser Particle analyzer results for sample 01

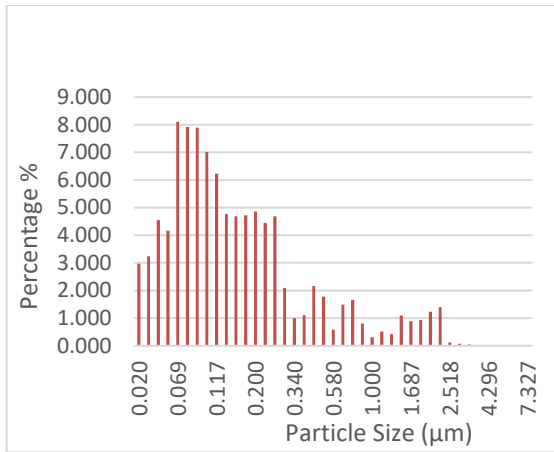


Figure 6. Laser Particle analyzer results for sample 02

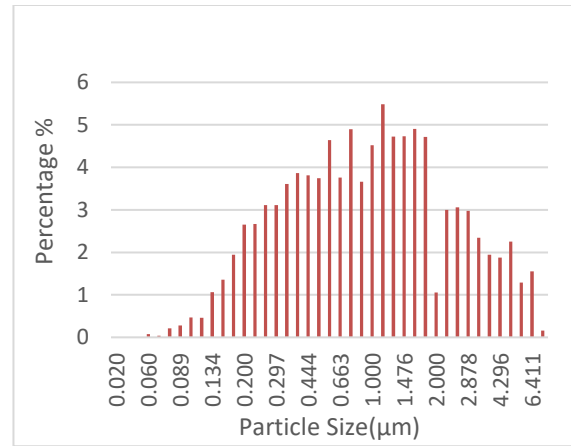


Figure 9. Laser Particle analyzer results for sample 05

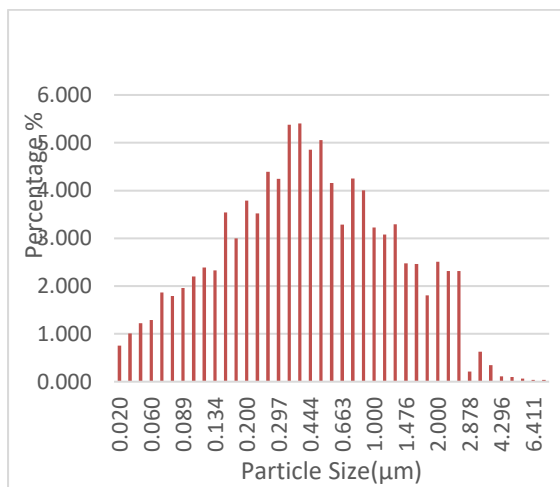


Figure 7. Laser Particle analyzer results for sample 03

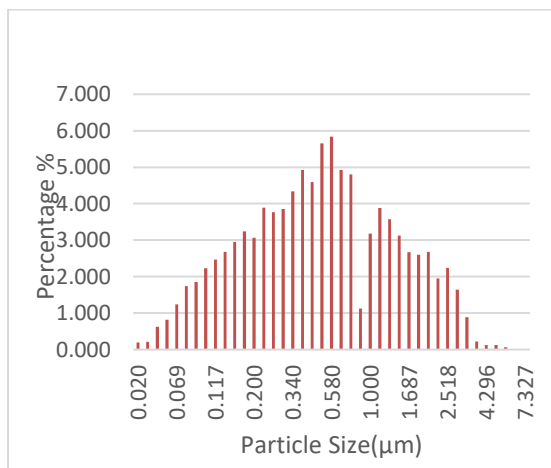


Figure 8. Laser Particle analyzer results for sample 04

Table 2. Parameters for particle size distributions obtained by Laser particle analyser

Sample	Mode particle Size (nm)	Mean particle Size (nm)	Standard Deviation (nm)
1	50	170	267
2	69	286	465
3	389	704	744
4	580	770	769
5	1130	1408	1394

The SEM study reveals the formation of well-dispersed rod-shaped nanoparticles in the samples. Figure 10 clearly shows the formation of nanoparticles in the first sample. They are nearly rod-shaped and have a compromised size with laser particle analyser. The EDS analysis revealed the presence of Ca, P, and O in the sample with Ca/P molar ratio of 1.69.

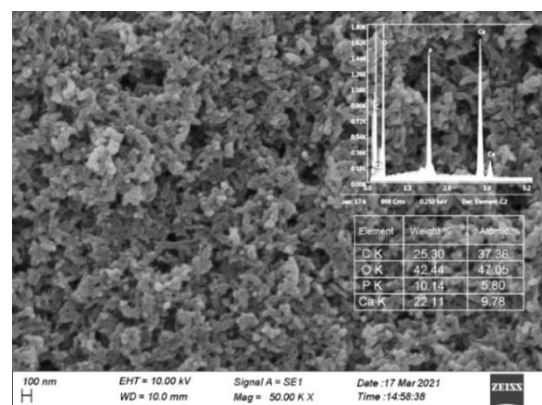


Figure 10. SEM image of hydroxyapatite particles synthesized in first sample

Synthesized nano hydroxyapatite controlled by supersaturation can be particularly used in

preventive, restorative and degenerative dentistry due to its unique properties, such as the remineralizing effect on initial enamel lesion, good results on the sensitivity of teeth, ability to bond to the bone chemically, non-toxicity nor inflammation, stimulation of bone growth through the direct action of osteoblasts. Specially the synthesized nano level and purity of hydroxyapatite suit the applications in periodontology, oral and maxillofacial surgery, oral implantology, orthopaedics with the above-mentioned properties in the nano domain and the osteoconductive behaviour which provides the better osteointegration strengthening the bone to implant connection. Synthesized nano powder from other methods does not give higher purity which make it suitable for medical or biological application and micro range particle domain does not provide the significant osteo integrative properties. Simply, the nano range gives the highest surface area so that protein and other fragments bind easily.

IV. CONCLUSION

In summary, the wet chemical precipitation method could fabricate stoichiometric HA nanoparticles with rod shaped morphology. This is very versatile method to synthesize HA nanoparticles in large quantities with reproducibility. The advantage of this method is that it gives water soluble biproducts which can easily be washed to recover high purity nano hydroxyapatite for biological applications. This study basically tailored the particle size to supersaturation of the precursor solution. Because of electrostatic interactions in ionic solutions, the higher precursor concentrations always do not give the higher supersaturation. Therefore, the need of ionic strength consideration for a synthesis was highly noted. The nucleation rate which was mentioned to be inversely proportional to the induction time contributed mainly to the size of the nano particles being synthesized. Higher nucleation rates, in other words lower induction time gave the smaller size and narrow distribution. Although the increased supersaturation is better for the nano particle synthesis, when concentrations are too high, the obtained size distribution, can be broader promoting the growing phase. In this study, it is learnt that supersaturation must be optimum for a narrow particle distribution.

REFERENCES

C. Guzmán Vázquez, C. Pina Barba, and N. Munguía, (2005), Stoichiometric hydroxyapatite obtained by precipitation and sol gel processes, revista mexicana de fisica 51 (3), 284-293.

Gross, K.A., Berndt, C.C., Stephens, P. and Dinnebier, R. (1998), "Oxyapatite in hydroxyapatite coatings", *J. Mater. Sci.*, 33(15), 3985-3991.

Liu, D.M., Troczynski, T. and Tseng, W.J. (2001), "Water-based sol-gel synthesis of hydroxyapatite: process development", *Biomaterial*, 22(13), 1721-1730.

Morales, J.G., Burgues, J.J., Boix, T., Fraile, J. and Clemente R.R. (2001), "Precipitation of stoichiometric hydroxyapatite by a continuous method", *Cryst. Res. Technol.*, 36(1), 15-26.

Mp Ferraz Fj Monteiro C.M. Manuel (2004), Hydroxyapatite nanoparticles: A review of preparation methodologies

Naruporn M, (2008), Nano-size Hydroxyapatite Powders Preparation by Wet-Chemical Precipitation Route, *Metals, Materials and Minerals*, 18(1),15-20.

Nguyen T. K. Thanh, * N. Maclean, and S. Mahiddine (2014), Mechanisms of Nucleation and Growth of Nanoparticles in Solution, 114,7610-7630.

S. U. Adikary, J. M. N. Jayaweera, and G. A. Sewvandi (2011), Synthesis and Characterization of Hydroxyapatite to be used as a Biomaterial

Sahebali Manafi, Seyyed Hossein Badiie, (2008), Effect of Effect of Ultrasonic on Crystallinity of Nano-Hydroxyapatite via Wet Chemical Method, *Pharmaceutical Sciences*, 4(2), 163-168.

Sudip Mondal, Apurba Dey, Umapada Pal (2016), Low temperature wet-chemical synthesis of spherical hydroxyapatite nanoparticles and their in-situ cytotoxicity study, 295-307.

Tampieri, A., Celotti, G., Szontagh, F. and Landi, E. (1997), "Sintering and characterization of HA and TCP bio ceramics with control of their strength and phase purity", *J. Mater. Sci. Mater. Med.*, 8(1), 29-37.